A [Cyclentetrakis(methylene)]tetrakis[2-hydroxybenzamide] Ligand That Complexes and Sensitizes Lanthanide(III) Ions

by **Anthony D'Aléo**[a]), **Jide Xu**[a]), **King Do**[b]), **Gilles Muller**[b]), and **Kenneth N. Raymond***[a])

[a]) Chemical Sciences Division, Lawrence Berkeley National Laboratories, Berkeley, CA 94720, and Department of Chemistry, University of California, Berkeley, CA 94720-1460, USA (raymond@socrates.berkeley.edu)

[b]) Department of Chemistry, San José State University, San José, CA 95192-0101, USA

Dedicated to Professor *Jean-Claude Bünzli* on the occasion of his 65th birthday

The synthesis of the cyclen derivative $H_4\mathbf{L^1}\cdot 2\,HBr$ containing four 2-hydroxybenzamide groups is described. The spectroscopic properties of the Ln^{III} conplexes of $\mathbf{L^1}$ (Ln = Gd, Tb, Yb, and Eu) reveal changes of the UV/VIS-absorption, circular-dichroism-absorption, luminescence, and circularly polarized luminescence spectra. It is shown that at least two metal-complex species are present in solution, whose relative amounts are pH dependent. At pH > 8.0, an intense long-lived emission is observed (for [Tb$\mathbf{L^1}$] and [Yb$\mathbf{L^1}$]), while at pH < 8.0, a weaker, shorter-lived species predominates. Unconventional Ln^{III} emitters (Pr, Nd, Sm, Dy, and Tm) were sensitized in basic solution, both in the VIS and in the near-IR, to measure the emission of these ions.

Introduction. – Luminescent lanthanide complexes have attracted much recent attention because of their use and potential in a wide variety of applications such as biofluoroimmunoassays [1][2], sensors [3–7], light-emitting diodes [8–10], and waveguide amplifiers for lasers [11–17]. In most of the cases, luminescent lanthanide complexes consist of a lanthanide ion attached to a chelating chromophore which transfers the excitation energy to the lanthanide ion, which must be protected from H_2O coordination to avoid quenching. The presence of this chromophore overcomes the limitation of an intrinsically small molar absorption coefficient (ε) for the metal by using a strongly absorbing organic ligand. This light-harvesting phenomenon is known as the *antenna effect* and, compared to the bare cations, increases the brightness (defined as the product of the luminescence quantum yield and of the molar absorption coefficient) and the luminescence lifetimes of the lanthanide ions, which are highly sensitive to the local environment and quenched by overtones of X–H vibrations, where X = O, N, C.

At the molecular level, the strong paramagnetism of these ions has led to important applications in NMR shift reagents applicable in 3D-protein-structure determination, for example [18]. The ligand-field splitting of Ln^{III} can also be used to determine changes in coordination geometry around the lanthanide ion [19–23]. In such cases, the luminescence pattern can be used to determine or indicate a change in the geometry of the binding atoms about the lanthanide center. In addition, chiral ligands allow the use of techniques such as circular-dichroism (CD) absorption or circularly polarized

luminescence (CPL) that provide insight into the chiral-ligand conformations (number of species present as well as differentiation of those species).

We report herein the synthesis of a ligand $H_4\mathbf{L^1}\cdot 2\,HBr$ composed of a cyclen (=1,4,7,10-tetraazacyclododecane) scaffold with four appended 2-hydroxybenzamide groups (*Scheme*). The free ligand $H_4\mathbf{L^1}\cdot 2\,HBr$ was complexed to a series of Ln^{III} (Ln = Gd, Tb, Yb, Eu, Pr, Nd, Sm, Dy, and Tm). A detailed study on the spectroscopic properties of the uncomplexed ligand as well as of its Gd, Tb, Yb, and Eu complexes shows the presence of two emissive complex species whose relative amounts depend on the pH of the base/buffer used. The dominant species at high pH luminesces intensely and exhibits a long luminescence lifetime, while the dominant species at mildly acidic pH is less emissive and has a shorter lifetime. Assignment of the emissive transitions for other unconventional Ln^{III} (Ln = Pr, Nd, Sm, Dy, and Tm) is also presented.

Scheme. *Preparation of the Ligand* $H_4\mathbf{L^1}\cdot 2\,HBr$

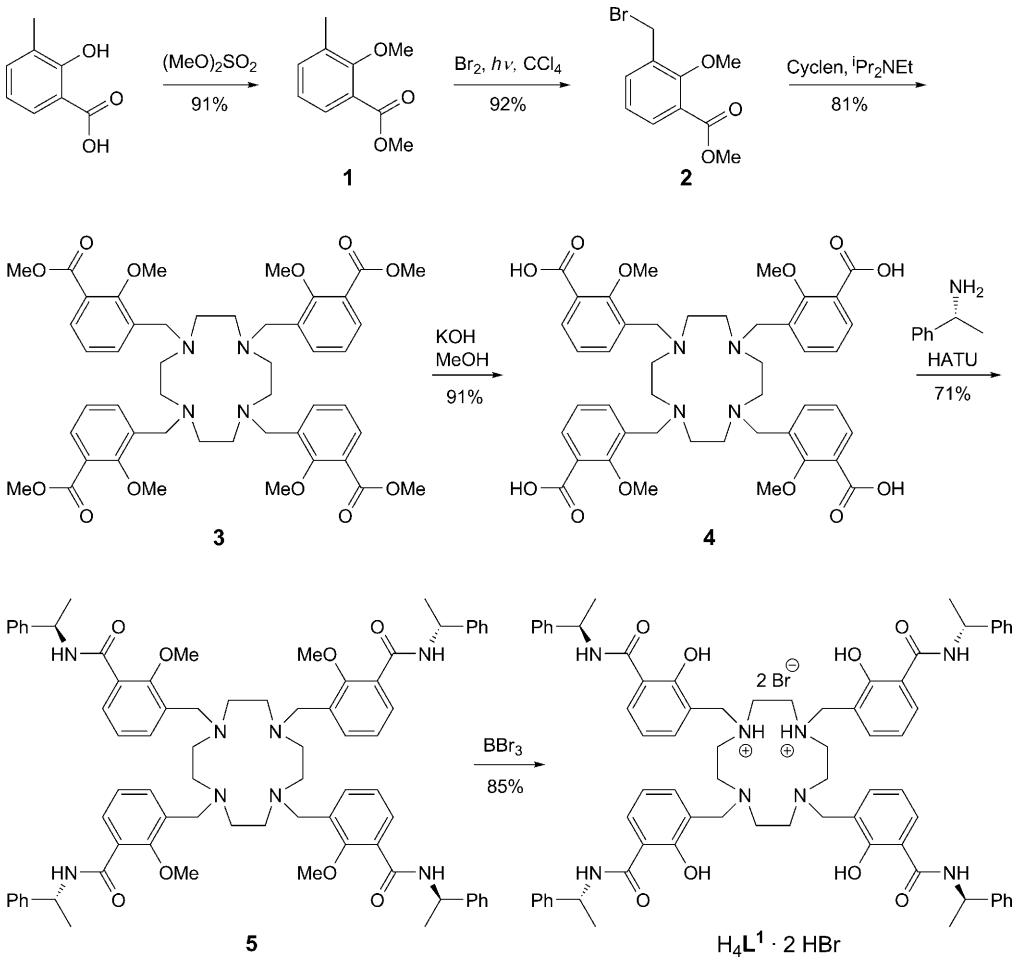

Experimental. – 1. *General.* Thin-layer chromotography (TLC): precoated silica gel *60* F_{254} plates. Flash chromatography (FC): *EM-Science* silica gel *60* (SiO_2; 230–400 mesh). NMR Spectra: *Bruker-AM-300* or *-DRX-500* spectrometers, at 300 (75) and 500 (125) MHz for ^1H (or ^{13}C), resp.; δ(H) or δ(C) in ppm rel. to the solvent resonances, taken as δ(H) 7.26 (δ(C) 77.0) and δ(H) 2.49 (δ(C) 39.5), resp., for $CDCl_3$ and (D_6)DMSO, coupling constants *J* in Hz. Fast-atom bombardment mass spectra (FAB-MS): 3-nitrobenzyl alcohol (NBA) or thioglycerol/glycerol (TG/G) as the matrix; in *m*/*z* (rel. %). Elemental analyses were performed by the Microanalytical Laboratory, University of California, Berkeley, CA.

2. *Syntheses. Methyl 2-Methoxy-3-methylbenzoate* (**1**). To a mixture of 3-methylsalicylic acid (200 g, 1.32 mol), anh. K_2CO_3 (500 g, 3.6 mol), and dry acetone (3.5 l) (5 l round-bottom flask), dimethyl sulfate ($(MeO)_2SO_2$; 210 ml, 2.2 mol) was added in several portions. The mixture was stirred for 2 d (TLC monitoring) and then heated under reflux overnight. The mixture was then filtered and the filtrate concentrated: **1** (215 g, 91%). Pale yellow thick oil: ^1H-NMR (500 MHz, $CDCl_3$, 25°): 2.26 (*s*, Me); 3.78 (*s*, MeO); 3.85 (*s*, MeO); 6.98 (*t*, $^3J = 7.5$, 1 arom. H); 7.27 (*d*, $^3J = 7.5$, 1 arom. H); 7.58 (*d*, $^3J = 7.5$, 1 arom. H). ^{13}C-NMR (125 MHz, $CDCl_3$, 25°): 15.7; 51.8; 61.2; 123.3; 124.4; 128.9; 132.5; 134.88; 158.2; 166.6.

Methyl 3-(Bromomethyl)-2-methoxybenzoate (**2**). A 1000-watt halogen-tungsten lamp was placed in an upright position about 3 cm from a 500 ml flask containing **1** (0.05 mol) and benzene (80 ml). The soln. was gently refluxed and irradiated while 0.05 mol of Br_2 in 80 ml of benzene was added at such a rate that a red color persisted at all times. The reaction was judged complete when all Br_2 was added and the red Br_2 color had disappeared: **2** (92%). ^1H-NMR (500 MHz, $CDCl_3$, 25°): 3.92 (*s*, MeO); 3.96 (*s*, MeO); 4.58 (*s*, CH_2Br); 6.86 (*t*, $^3J = 7.8$, 1 arom. H); 7.55 (*dd*, $^3J = 7.5$, 1.8, 1 arom. H); 7.81 (*dd*, $^3J = 7.5$, $^4J = 1.8$, 1 arom. H). ^{13}C-NMR (125 MHz, $CDCl_3$, 25°): 27.4; 52.3; 62.8; 123.9; 124.7; 132.4; 132.8; 135.19; 158.5; 166.1.

Tetramethyl 3,3′,3″,3‴-[1,4,7,10-Tetraazacyclododecane-1,4,7,10-tetrayltetrakis(methylene)]tetrakis[2-methoxybenzoate] (**3**). To a soln. of cyclen (300 mg, 1.74 mmol) in dry MeCN (30 ml) were added *N*,*N*-diisopropylethylamine (3.1 ml, 18 mmol) and **2** (2.1 g, 8.1 mmol) consecutively. The mixture was warmed to 60° under N_2 for 24 h. The white precipitate was filtered, washed with MeCN (3 × 5 ml), and dried *in vacuo*: **3** (81%). Beige solid. ^1H-NMR (500 MHz, $CDCl_3$, 25°): 2.73 (*s*, 16 H, cyclen-CH_2); 3.55 (*s*, 4 benzylic CH_2); 3.72 (*s*, 4 MeO); 3.98 (*s*, 4 MeO); 6.87 (*t*, $^3J = 7.5$, 4 arom. H); 7.63 (*d*, $^3J = 7.5$, 4 arom. H); 7.91 (*d*, $^3J = 7.5$, 4 arom. H). ^{13}C-NMR (125 MHz, $CDCl_3$, 25°): 52.1; 53.2; 53.5; 62.0; 123.4; 123.9; 134.3; 134.5; 158.2; 166.7. FAB-MS (pos.): 885.5 ($[M+H]^+$, $C_{48}H_{61}N_4O_{12}^+$; calc. 885.4).

3,3′,3″,3‴-[1,4,7,10-Tetraazacyclododecane-1,4,7,10-tetrayltetrakis(methylene)]tetrakis[2-methoxybenzoic Acid] (**4**). To a stirred soln. of **3** (445 mg, 0.5 mmol) in MeOH (30 ml) was added 10% aq. KOH soln. (1 ml). The mixture was stirred for 16 h. The volatiles were evaporated, and the residue was dissolved in H_2O. The soln. was neutralized with 6N HCl, and the solid product was collected and dried *in vacuo*: **4** (91%). Beige solid. ^1H-NMR (300 MHz, D_2O/NaOD, 25°): 2.80 (br. *s*, 8 H, cyclen-CH_2); 3.67 (*s*, 4 MeO); 2.75 (br. *s*, 4 benzylic CH_2); 7.15 (*t*, $^3J = 7.2$, 4 arom. H); 7.51 (*d*, $^3J = 6.9$, 4 arom. H); 7.65 (*d*, $^3J = 7.2$, 4 arom. H); 13.04 (br. *s*, 4 COOH). FAB-MS (pos.): 773 ($[M+H]^+$, $C_{40}H_{45}N_4O_{12}^+$; calc. 773.3).

3,3′,3″,3‴-[1,4,7,10-Tetraazacyclododecane-1,4,7,10-tetrayltetrakis(methylene)]tetrakis[2-methoxy-N*-[(1*R*)-1-phenylethyl]carboxamide]* (**5**). To a stirred soln. of **4** (77 mg, 1 mmol) in dry DMF (5 ml), which was cooled in an ice bath, (+)-(1*R*)-1-phenylethanamine (0.5 ml, 4.1 mmol) was added under N_2. The cold mixture was treated with HATU (= *O*-(7-azabenzotriazol-1-yl)-*N*,*N*,*N*′,*N*′-tetramethyluronium hexafluorophosphate; 0.77 g, 2 mmol) and *N*,*N*-diisopropylethylamine (1 ml, 5.7 mmol) successively. The mixture was stirred for 7 h, then the solvent was evaporated. The residue was partitioned between CH_2Cl_2 (20 ml) and 1M aq. HCl (2 × 20 ml), the org. phase concentrated, and the residue purified by FC (SiO_2, gradient 3 → 7% MeOH/CH_2Cl_2): **5** (71%). White foam. ^1H-NMR (300 MHz, $CDCl_3$, 25°): 1.56 (*s*, 4 Me); 2.83 (br. *s*, 8 cyclen-CH_2); 3.46 (*s*, 4 MeO); 3.65 (*s*, 4 benzylic CH_2); 7.03 (*t*, $^3J = 8.0$, 4 arom. H); 7.20–7.40 (*m*, 20 arom. H); 7.48 (*d*, $^3J = 8.1$, 4 arom. H); 7.84 (*d*, $^3J = 7.8$, 4 arom. H). ^{13}C-NMR (125 MHz, $CDCl_3$, 25°): 21.2; 39.4; 49.7; 51.2; 62.4; 124.2; 125.9; 127.1; 128.4; 128.8; 131.2; 134.1; 142.9; 156.5; 164.1; 170.4. FAB-MS (pos.): 1241.6 ($[M+H]^+$, $C_{76}H_{89}N_8O_8^+$; calc. 1241.7).

3,3′,3″,3‴-[1,4,7,10-Tetraazacyclododecane-1,4,7,10-tetrayltetrakis(methylene)]tetrakis[2-hydroxy-N*-[(1*R*)-1-phenylethyl]carboxamide] Hydrogenbromide (1:2)* ($H_4\mathbf{L^1}2\cdot HBr$). To a stirred soln. of **5** (445 mg, 0.5 mmol) in dry CH_2Cl_2 (30 ml) was added an excess of BBr_3 (1 ml) with cooling under N_2. The mixture was stirred for 48 h. The volatiles were evaporated, and the residue was quenched with MeOH

(150 ml). The MeOH soln. was refluxed gently in an open round-bottom flask overnight. The MeOH soln. was then boiled with H_2O for 6 h. The product precipitated upon cooling and was dried *in vacuo:* $H_4\mathbf{L^1}\cdot 2$ HBr (85%). Beige solid. ^{1}H-NMR (300 MHz, $CDCl_3$, 25°): 1.46 (*s*, 4 Me); 2.80–3.30 (br. *s*, 8 cyclen-CH_2); 3.98 (*s*, 4 benzylic CH_2); 5.18 (*m*, 4 CH); 6.18 (*t*, $^3J = 7.5$, 1 arom. H); 6.99 (*t*, $^3J = 8.5$, 3 arom. H); 7.20–7.40 (*m*, 20 arom. H); 7.58 (*d*, $^3J = 7.2$, 4 NH); 7.95 (*d*, $^3J = 8.1$, 1 arom. H); 8.09 (*d*, $^3J = 7.8$, 3 arom. H). 9.20 (*d*, $^3J = 7.8$, 1 arom. H); 9.29 (*d*, $^3J = 8.4$, 3 arom. H). FAB-MS (pos.): 1185.6 ($[M+H]^+$, $C_{72}H_{81}N_8O_8^+$; calc. 1185.6). Anal. calc. for $C_{72}H_{80}N_8O_8\cdot 2$ HBr (1347.28): C 64.19, H 6.13, N 8.32; found: C 64.23, H 6.43, N 8.14.

{Cyclenetetrakis(methylene)tetrakis[2-hydroxybenzamidato(1–)}lanthanide Pyridinium Dibromide Complex. Ligand $H_4\mathbf{L^1}\cdot 2$ HBr (1 equiv.) was dissolved in MeOH (3 ml) with three drops of pyridine. Lanthanide(III) chloride hexahydrate (1 equiv.) in MeOH (3 ml) was added. The soln. was heated to reflux temp. during 4 h, and then left to cool to r.t. Slow evaporation of the MeOH at r.t. for one night afforded a precipitate of the complex, which was collected by filtration.

[GdH_3($\mathbf{L^1}$)]Br_2. Yield 17%. Anal. calc. for $C_{81}H_{90}GdN_9O_8\cdot 2$ HBr $\cdot 9$ H_2O (1798.85): C 51.98, H 5.88, N 6.74; found: C 51.98, H 5.57, N 6.84.

[TbH_3($\mathbf{L^1}$)]Br_2. Yield 23%. Anal. calc. for $C_{81}H_{90}N_9O_8Tb\cdot 2$ HBr $\cdot 9$ H_2O (1800.52): C 51.96, H 5.81, N 6.73; found: C 52.07, H 5.98, N 6.71.

[YbH_3($\mathbf{L^1}$)]Br_2. Yield 22%. Anal. calc. for $C_{81}H_{90}N_9O_8Yb\cdot 2$ HBr $\cdot 15$ H_2O (1922.73): C 48.38, H 6.16, N 6.27; found: C 48.09, H 5.99, N 6.33.

3. *Optical Spectroscopy.* UV/VIS Absorption spectra: *Varian-Cary-300* double beam absorption spectrometer. Circular-dichroism spectra: *Jasco-J-810* spectropolarimeter. Circularly polarized luminescence and total luminescence spectra were recorded on an instrument described previously [24][25] operating in a differential photon-counting mode. The light source for indirect excitation was a continuous-wave 450 W Xe arc lamp from a *Spex-FluoroLog-2* spectrofluorometer, equipped with excitation and emission monochromators with dispersions of 4 nm/mm (*Spex*, *1681B*). Selective excitation of Tb^{III} was accomplished with either a *Coherent Innova-70* or *Coherent Sabre TSM 15*. The optical-detection system consisted of a focusing lens, long pass filter, and 0.22 m monochromator. The emitted light was detected by a cooled *EMI-9558B* photomultiplier tube operating in photon-counting mode. All measurements were performed with quartz cuvettes with a path length of 0.4 or 1.0 cm. Emission spectra were acquired with a *Horiba-Jobin-Yvon-IBH-FluoroLog-3* spectrofluorimeter, equipped with 3-slit double-grating excitation and emission monochromators (2.1 nm/mm dispersion, 1200 grooves/mm). Spectra were reference-corrected for both the excitation-light-source variation (lamp and grating) and the emission-spectral response (detector and grating). Luminescence lifetimes were determined with a *Horiba-Jobin-Yvon-IBH-FluoroLog-3* spectrofluorimeter, adapted for time-correlated single-photon-counting (TCSPC) and multichannel scaling (MCS) measurements. A sub-microsecond Xe flashlamp (*Jobin Yvon*, *5000XeF*) was used as the light source, with an input pulse energy (100 nF discharge capacitance) of *ca.* 50 mJ, yielding an optical-pulse duration of less than 300 ns at FWHM. Spectral selection was achieved by passage through the same double-grating excitation monochromator. Emission was monitored perpendicular to the excitation pulse, again with spectral selection achieved by passage through the double-grating emission monochromator (2.1 nm/mm dispersion, 1200 grooves/mm). A thermoelectrically cooled single-photon-detection module (*Horiba Jobin Yvon IBH*, *TBX-04-D*) incorporating a fast-rise-time photomultiplier tube (PMT), a wide-bandwidth preamplifier, and a picosecond constant-fraction discriminator was used as the detector. Signals were acquired with an *IBH-DataStation-Hub* photon-counting module, and data analysis was performed with the commercially available DAS-6 decay-analysis software package from *Horiba Jobin Yvon IBH*. Goodness of fit was assessed by minimizing the reduced chi squared function, χ^2, and a visual inspection of the weighted residuals. Each trace contained at least 10000 points, and the reported lifetime values resulted from at least three independent measurements. Typical sample concentrations for both absorption and fluorescence measurements were *ca.* 10^{-5}–10^{-6} M and 1.0 cm cells in quartz *Suprasil* or equivalent were used for all measurements. Quantum yields were determined by the optically dilute method (with optical density < 0.1) with *Eqn. 1*, where A is the absorbance at the excitation wavelength (λ), I is the intensity of the excitation light at the same wavelength, n is the refractive index, and D is the integrated luminescence intensity. The subscripts 'x' and 'r' refer to the sample and reference, resp. For

quantum-yield calculations, an excitation wavelength of 340 nm was utilized for both the reference and sample, hence the $I(\lambda_r)/I(\lambda_x)$ term is removed. Similarly, the refractive indices term, n_x2/n_r2, was taken to be identical for the aq. reference and sample solns. Hence, a plot of integrated emission intensity (*i.e.*, D_r) *vs.* absorbance at 340 nm (*i.e.*, $A_r(\lambda_r)$) yields a linear plot with a slope which can be equated to the reference quantum yield Φ_r. Quinine sulfate in 0.5M (1.0N) H_2SO_4 was used as the reference ($\Phi_r = 0.546$). By analogy, for the sample, a plot of integrated emission intensity (*i.e.*, D_x) *vs.* absorbance at 340 nm (*i.e.*, $A_x(\lambda_x)$) yields a linear plot, and Φ_x can then be evaluated. The values reported in this paper are the average of four independent measurements. For Yb^{III}, since there is no reliable NIR reference, the luminescence quantum yield were measured one resp. to the other fixing, arbitrary, the value of the lowest pH measured to 1.

$$\Phi_x/\Phi_r = [A_r(\lambda_r)/A_x(\lambda_x)][I(\lambda_r)/I(\lambda_x)][n_x2/n_r2][D_x/D_r] \quad (1)$$

Synthesis. – The ligand was synthesized by a six-step synthesis starting from commercially available 3-methylsalicylic acid (*Scheme*). First, the phenolic and carboxylic acid groups were protected by Me groups with $(MeO)_2SO_2$ ($\rightarrow$**1**). Subsequently, the Me group was oxidized to give the bromomethyl derivative **2**. This synthon readily reacted with cyclen in basic medium yielding **3**. This protected ester was then saponified ($\rightarrow$**4**), and the chiral amino group was introduced by amidation in the presence of HATU ($\rightarrow$**5**). Finally, the phenolic methyl ether functions were deprotected with BBr_3 yielding the desired ligand $H_4\mathbf{L^1} \cdot 2\,HBr$ in rather good yield (32% overall).

The metal complexes were prepared in the presence of an excess of pyridine as base by refluxing 1 equiv. of ligand with one equiv. of $LnCl_3 \cdot 6\,H_2O$ in MeOH for 12 h. The resultant complexes were precipitated by adding Et_2O, washed thoroughly with pentane and cold Et_2O, and dried before submission to elemental analysis. All complexes analyzed fit with a $[LnH_3(\mathbf{L^1})]Br_2$ complex formula with the bromide counterion introduced from the ligand deprotection strategy. The Yb complex of $H_2\mathbf{L^2}$ (*Fig. 1*) was made *in situ* by adding 0.5 equiv. of $YbCl_3 \cdot 6\,H_2O$ in MeOH soln. as described for Tb^{III} derivatives [21]. The full characterization of the ligands and complexes and synthetic details are reported in the *Exper. Part*.

The free ligand $H_4\mathbf{L^1}$ contains twelve coordinating atoms (four O-atoms from the phenol moiety, four C=O groups from the benzamide moiety, and the four N-atoms

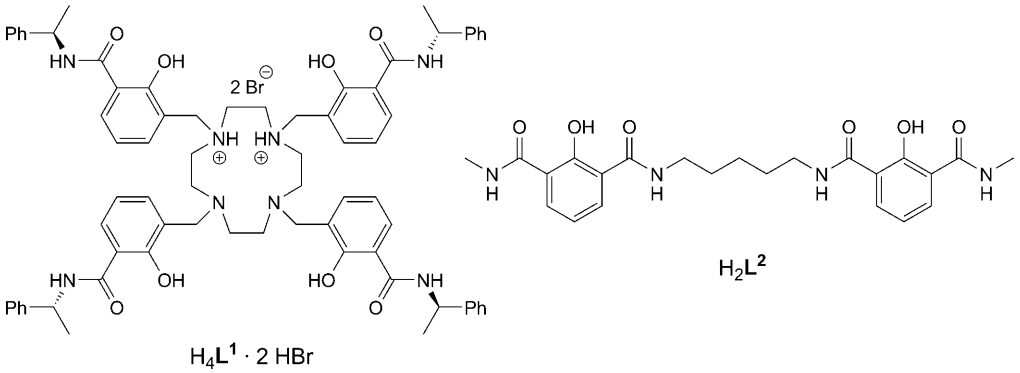

Fig. 1. *Studied ligand and its model* $H_2\mathbf{L^2}$

from the cyclen backbone), and possesses eight distinct pK_a values, four belonging to the cyclen scaffold and four belonging to the 2-hydroxybenzamide (phenol/phenolate) moieties. In the presence of lanthanide ions, $H_4\mathbf{L^1}\cdot 2\,HBr$ is expected to form [ML] complexes with a coordination number of eight (CN = 8) as confirmed by elemental analysis of the isolated lanthanide complexes. Furthermore, the presence of sterically hindered groups at the amide groups can be useful to protect the metal center from the local environment.

Results and Discussion. – Since the complexes were not stable in aqueous solution, the spectroscopic properties of $\mathbf{L^1}$, [Gd($\mathbf{L^1}$)], [Tb($\mathbf{L^1}$)], [Yb($\mathbf{L^1}$)], and [Eu($\mathbf{L^1}$)][1]) were carried out in MeOH solution where the stability was found to be higher. To control the basicity of the MeOH solutions, different organic bases of known pK_a values were used.

1. *Ligand.* The UV/VIS absorption spectra of the ligand $\mathbf{L^1}$ in MeOH in the presence of various bases with pK_as ranging from 0.2 to 14.0 are plotted in *Fig. 2,a*, whereas the data are reported in *Table 1*. As can be seen, the molar absorption coefficients vary from *ca.* 19000 to 23500 $M^{-1}\cdot cm^{-1}$ and are in good agreement with those of $[Tb(\mathbf{L^2})_2]^-$ (19300–26500 $M^{-1}\cdot cm^{-1}$) [21]. This is consistent with the four benzamide units branched *via* a CH_2 linker on the cyclen moiety. Of special importance is that the absorption maximum is blue-shifted from 335 nm in highly basic media (pH from 8.3 to 14.0) to 305 nm (pH below 6.0) with an isosbestic point at *ca.* 320 nm. By plotting the pH dependence of the molar absorption coefficients at 305 and 335 nm (*Fig. 2,b*), one can see the presence of a long transition between 4.8 and 11.2, which strongly suggests the presence of numerous protonations of $\mathbf{L^1}$.

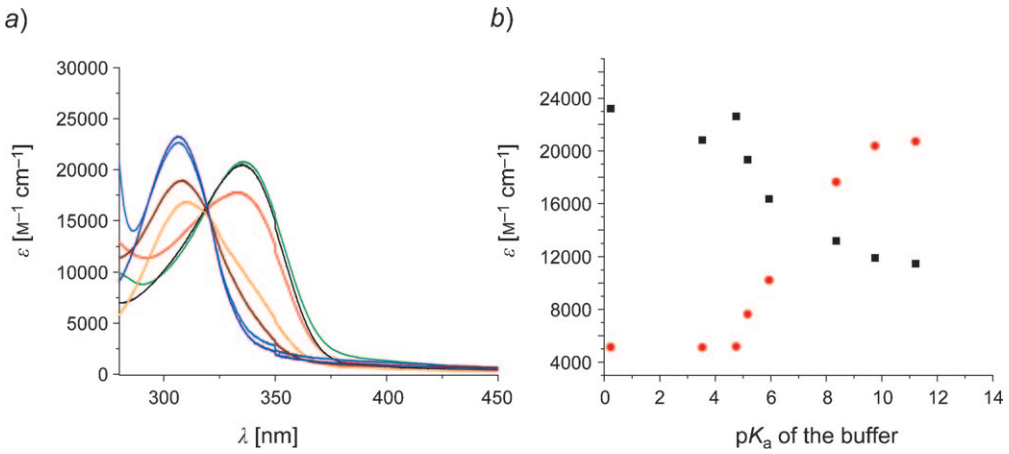

Fig. 2. a) *UV/VIS Absorption spectra of* $\mathbf{L^1}$ *as a function of the* pK_a *of the base used* (CF_3COOH (violet line), $ClCH_2COOH$ (blue line), pyridine (brown line), $N(CH_2CH(Me)OH)_3$ (orange line), *sym*-collidine (red line), Et_3N (green line), piperidine (black line)). b) *Evolution of the UV/VIS absorption molar absorption coefficient of* $\mathbf{L^1}$ *in MeOH at 306 nm* (■) *and 335nm* (●) *as a function of the* pK_a *of the base used.*

[1]) For convenience, the short forms [Ln($\mathbf{L^1}$)] are used for $[LnH_3(\mathbf{L^1})]Br_2$. $H_4\mathbf{L^1}\cdot 2\,HBr$ in solution is denoted by $\mathbf{L^1}$.

Table 1. *Optical Properties of* $\mathbf{L^1}$ *in MeOH at Room Temperature and at 77 K in the Presence of Different Acids or Bases*

Acid/base	pK_a	S_1			T_1		77 K
		λ_{abs} [nm] (ε [M^{-1} cm^{-1}])	λ_{em} [nm]	ϕ_{em}	λ_{em} [nm]	ϕ_{em}	λ_{em} [nm]
CF_3COOH	0.2	307 (23240)	–[a])	–[a])	434	0.152	–[b]), 422
$ClCH_2COOH$	2.9	307 (22490)	–[a])	–[a])	433	0.163	–[b]), 428
$MeOCH_2COOH$	3.5	308 (18940)	–[a])	–[a])	430	0.149	361, 417
AcOH	4.8	307 (22440)	–[a])	–[a])	434	0.225 (0.243)	361, 417
Pyridine	5.2	307 (19300)	–[a])	–[a])	–[a])	0.097	–[b])
$N(CH_2CH(Me)OH)_3$	5.9	310 (16830)	–[a])	–[a])	437	0.113	373, 427
sym-Collidine	7.4	334 (19830)	–[a])	–[a])	436	0.108	362, 429
Morpholine	8.4	334 (20780)	385[c])	–[c])	430	0.100	378, 421
Et_3N	9.8	335 (20570)	386[c])	–[c])	422	0.224	385, 420
Piperidine	11.2	336 (20820)	411	–[c])	–[a])	0.234	378, –[b])
Bu_4NOH	14.0	335 (23620)	408	–[c])	–[a])	0.315	N/A

[a]) No signal observed. [b]) Undeterminable. [c]) Appears as a shoulder.

The luminescence spectra of $\mathbf{L^1}$ were measured in MeOH solutions. The quantum yields were determined with quinine hydrogensulfate in 1N H_2SO_4 as the standard and corrected for the different refractive indexes of the solvents [26]. Selected spectra are shown in Fig. S1a of the *Supplementary Information* (*S. I.*)[2]), and all the data are reported in *Table 1*. In acidic medium, only one broad emission band is observed, with a maximum at *ca.* 435 nm. This emission maximum is red-shifted compared to the maximum observed in the absorption spectra (100–130 nm *Stoke* shift). In basic medium, the same emission profile is observed with a shoulder on the blue side of the emission. This shoulder can be attributed to the emission band of the singlet excited state (with a small *Stokes* shift), while the main emission band at *ca.* 435 nm corresponds to the triplet excited state of $\mathbf{L^1}$. It should be noted that the observation of the unconventional emission from the triplet excited state at room temperature is due to the heavy-atom effect induced by the bromide salt of the ligand. This was confirmed by recording the emission spectra at 77 K (Fig. S2 of the *S. I.*[2])).

2. *Gadolinium.* Trivalent Gd-ion was chosen because of its similar electronic structure and size with Eu^{3+} ($4f^7$ *vs.* $4f^6$), but lacking an accessible metal-based low-energy electronic excited state (the lowest one, $^6P_{7/2}$, lies at 32224 cm^{-1}). As a result, one can expect the same kind of information found for the free ligand, but it will correspond to the positions of the excited singlet and triplet states of the ligand complexed to the Gd^{3+} ion. For instance, the molar absorption coefficients range from 19000 to 23500 $M^{-1} \cdot cm^{-1}$, whereas the absorption maxima are found between 305 and 325 nm in basic medium, with an isosbestic point at 313 nm (Fig. S3a of the *S. I.*[2])). These changes in the position of the absorption maxima between the free and complexed ligands confirm the formation of the complex.

The complex formation is also corroborated by the changes observed in the pH dependence of the UV/VIS absorption molar coefficient values (Fig. S3b of the *S. I.*[2])).

---

[2]) *Supplementary Information* (*S. I.*) is available upon request from *K. N. R.*

Unlike the free ligand (one protonation step, Fig. S1b of the *S. I.*[2])), the complexation of $\mathbf{L^1}$ to Gd^{III} showed two different protonation steps, observed between 4–5 and 7–8, respectively. In addition to the isosbestic point at 313 nm, there is also one at 341 nm that can be associated to the higher pH species.

As observed for the ligand, the emission spectra of [Gd($\mathbf{L^1}$)] are dependent on the pH determined by the bases used (Fig. S4a of the *S. I.*[2])). The main difference between $\mathbf{L^1}$ and its Gd^{III} complex was that the emission spectrum has a broad emission band at *ca.* 375 nm, corresponding to the singlet excited state, with a shoulder growing in at 435 nm (attributed to the triplet excited state) when the pH is decreased. It should be noted that the variation of the quantum yield cannot be taken into account since two different states are involved and the intersystem crossing rate changes with the conditions (Fig. S4b of the *S. I.*[2])).

At 77 K, despite a small residual emission arising from the singlet excited state, the emission spectra are mainly composed of a structured emission band located at *ca.* 430 nm (*Fig. 3*). The deconvolution of this triplet-excited-state emission band into a vibronic progression [27–29] of several overlapping *Gaussian* functions with separations of *ca.* 1000–1100 cm^{-1} led to the determination of a value of 24690 cm^{-1} for the triplet-excited-state energy. Such a high-energy triplet excited state should allow sensitization of many lanthanide ions, including Eu^{III}, Tb^{III}, Pr^{III}, Nd^{III}, Sm^{III}, Dy^{III}, or Tm^{III} (*vide infra*).

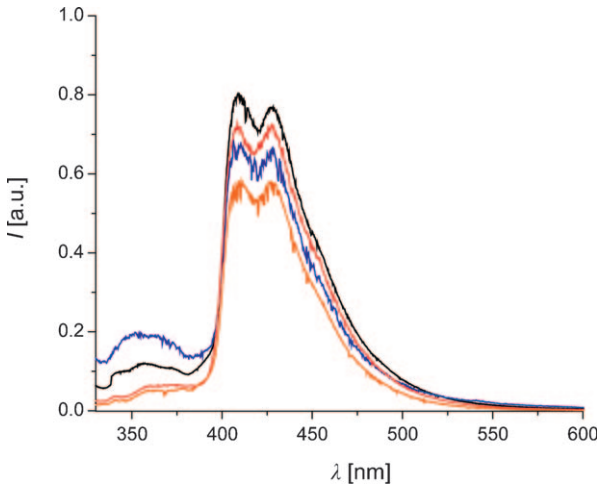

Fig. 3. *Luminescence spectra of [Gd($\mathbf{L^1}$)] in solid matrix* (77 K in a mixture MeOH/EtOH 1:4) *with selected bases or acids* (λ_{ex} 320 nm) (piperidine (black line), Et_3N (red line), morpholine (blue line), *sym*-collidine (orange line))

Finally, it must be emphasized that the Gd^{III} complex is unstable under acidic conditions, since identical absorption spectra and molar absorption coefficient values (within the experimental errors) were obtained for $\mathbf{L^1}$ and its Gd^{III} complex at room temperature (see *Tables 1* and *2*). A similar observation was noticed for the emission spectra recorded at 77 K (the two emission bands broaden to give similar spectra as for $\mathbf{L^1}$).

Table 2. *Optical Properties of* [Gd(**L1**)] *in MeOH at Room Temperature and at 77 K in the Presence of Different Acids or Bases*

Acid/Base	pK_a	S_1			T_1		77 K
		λ_{abs} [nm] (ε [M^{-1} cm^{-1}])	λ_{em} [nm]	ϕ_{em}	λ_{em} [nm]	ϕ_{em}	λ_{em} [nm]
CF_3COOH	0.2	307 (20050)	–[a])	–[a])	434	0.337	N/A
$ClCH_2COOH$	2.9	307 (19900)	–[a])	–[a])	432	0.336	–[a]), 431
$MeOCH_2COOH$	3.5	308 (19400)	387[b])	–[a])	430	0.301	–[b]), 429
AcOH	4.8	314 (16750)	–[a])	–[a])	431	0.151 (0.139)	–[a]), 431
Pyridine	5.2	317 (17800)	374	–[a])	428[b])	0.055 (0.059)	374, 435
$N(CH_2CH(Me)OH)_3$	5.9	321 (19300)	374	–[a])	428[b])	0.022	375, 428
sym-Collidine	7.4	323 (18600)	371	–[a])	432	0.020 (0.025)	373, 431
Morpholine	8.4	324 (21900)	377	–[a])	–[b])	0.021 (0.19)	377, –[a])
Et_3N	9.8	324 (21800)	376	–[a])	–[b])	0.023 (0.025)	375, –[a])
Piperidine	11.2	325 (22000)	374	–[a])	–[b])	0.020 (0.022)	374, –[b])
Bu_4NOH	14.0	328 (21950)		–[a])	–[b])	0.323	373, –[a])

[a]) No signal observed. [b]) Appears as a shoulder.

3. *Terbium.* Since the $^5D_4$ level is at 20500 cm^{-1} (Tb^{III} emitting excited state) and its next excited state ($^5G_6$) is 6000 cm^{-1} higher, Tb^{III} appears to be the ideal lanthanide to be sensitized by **L1**, based on the good match between the Tb^{III} and triplet-excited-state energies. The photophysical and chiroptical properties of [Tb(**L1**)] were studied by UV/VIS-absorption, CD-absorption, luminescence (luminescence quantum yield and luminescence lifetimes), and CPL spectroscopy at various pH values between 2.8 and 14.0. All the results are summarized in *Table 3*, and selected spectra are presented hereafter.

The UV/VIS profile of [Tb(**L1**)] is identical to the one of [Gd(**L1**)], with a shift of the absorption maximum from 305 nm to 325 nm when going from acidic to basic conditions (*Fig. 4*,*a*). The molar absorption coefficient values are *ca.* 20000 $M^{-1} \cdot cm^{-1}$, as observed for **L1** and [Gd(**L1**)]. As for [Gd(**L1**)], the UV/VIS spectra of [Tb(**L1**)] show two isosbestic points, and the pH dependence of the molar absorption coefficient values (*Fig. 5*,*a* and *b*) reveals the presence of two different pK_as (between 4–5 and *ca.* 7–8). The photophysical properties of the Gd^{III} and Tb^{III} complexes are then in good agreement and, more importantly, three species are present in solution. The change between these species seems to occur at pH values between 4–5 and 7–8.

As shown in *Fig. 4*,*b*, the luminescence spectra of [Tb(**L1**)] are different, depending on the base used and the resultant pH. In basic medium, the typical luminescence spectrum of the Tb^{III} ion can be observed with sharp line emission bands arising from the $^5D_4$ excited state on the ^7F_J manifold ground state. In an acidic medium, only the triplet-excited-state luminescence band can be observed, which suggests that the complex is not formed under these conditions. This is confirmed by the observation of the Tb- and ligand-centered emissions in the luminescence spectra of [Tb(**L1**)] under mild basic conditions (pH 5–6).

The luminescence quantum yield of the Tb complex can be calculated and separated from that of the triplet excited state. Thus, the dependence of the quantum yield of both excited states as a function of the pH of the base used can be followed

Table 3. *Optical Properties of* [Tb($\mathbf{L^1}$)] *in MeOH at Room Temperature and at 77 K in the Presence of Different Acids or Bases*

Acid/base	pK_a	Ln				T_1		77 K
		λ_{abs} [nm] (ε [M^{-1} cm^{-1}])	λ_{em} [nm]	ϕ_{em}	τ_{em} [ms]	λ_{em} [nm]	ϕ_{em}	τ_{em} [ms]
CF_3COOH	0.2	307 (19820)	–[a])	–[a])	–[a])	434	0.374	–[a])
$NH(CH_2CN)$	2.8	310 (21010)		0.025	2.08, 0.80	434	0.059	2.07, 0.73
$ClCH_2COOH$	2.9	306 (22080)	541	–[a])	2.06, 0.86	434	0.376	–[a])
$MeOCH_2COOH$	3.5	301 (23260)	541	–[a])	–[a])	434	0.059	2.05, 1.51
Benzoic acid	4.2	308 (N/A)	541	0.036	2.08, 0.96	434	0.349	2.08, 0.58
AcOH	4.8	316 (18400)	541	0.138	2.10, 0.96	434	0.062	2.05, 1.08
Pyridin-3-ol	4.9	323 (22180)	541	0.151	2.04, 0.81	434	0.060	2.09, 0.76
Pyridine	5.2	315 (24080)	541	0.215	2.15; 0.86	434	0.071	2.05, 1.16
1*H*-Benzimidazol	5.4	322 (22030)	541	0.301	2.03, 0.83	435	0.064	2.16, 0.93
1*H*-Imidazol	5.8	321 (N/A)	541	0.571	2.01	–[a])	–[a])	2.04
$N(CH_2CH(Me)OH)_3$	5.9	322 (20380)	541	0.541	2.11	–[a])	–[a])	2.11
2-Methyl-1*H*-imidazol	7.0	326 (N/A)	541	0.570	2.01	–[a])	–[a])	2.05
sym-Collidine	7.4	325 (22570)	541	0.535	2.12	–[a])	–[a])	2.08
Morpholine	8.4	325 (24390)	541	0.540	2.10	–[a])	–[a])	2.08
$MeN(CH_2CH_2OH)_2$	8.5	324 (25190)		0.569	1.99	–[a])	–[a])	2.09
$NH(CH_2CH_2OH)_2$	8.9	325 (25740)		0.579	2.02	–[a])	–[a])	2.06
Et_3N	9.8	325 (25880)	541	0.537	2.10	–[a])	–[a])	2.08
$MeOCH_2CH_2NH_2$	9.9	327 (N/A)	541	0.581	2.00	–[a])	–[a])	2.05
$NH(CH_2CH_2CH_2NH_2)_2$	10.7	325 (N/A)	541	0.569	2.06	–[a])	–[a])	2.10
Piperidine	11.2	325 (25540)	541	0.521	2.07	–[a])	–[a])	2.08
Bu_4NOH	14.0	326 (24370)	541	0.536	2.05	–[a])	–[a])	2.10

[a]) No signal observed.

(*Figs. 5c* and *d*). In the case of the Tb-centered emission, one can see that the luminescence quantum yield is low (3–4%) at low pH. A considerable increase is observed at pH *ca.* 4–5 (14–20%) and continues until it reaches its maximum (*ca.* 60%). On the other hand, the opposite effect can be observed when looking at the triplet-excited-state emission (*i.e.*, large and low quantum yields in acidic and basic media, resp.). This quenching of the triplet-excited-state emission as the Tb-centered luminescence increases reflects the efficiency of the energy transfer (poor and good efficiencies under acidic and basic conditions, resp.), and that the separation of these two species is possible in the presence of bases of appropriate strength.

This luminescence study allows us to conclude that there are at least two different species depending on the pH of the solution, resulting in changes in the emission efficiency.

Another way to observe the number of species is to measure the luminescence lifetime of the Tb-centered emission. At room temperature, one monoexponential decay of *ca.* 2.1 ms can be found above pH *ca.* 6, while below this pH, a second component can be detected with a shorter luminescence lifetime of *ca.* 800 μs (Fig. S5a of the *S. I.*[2]) and *Table 3*). The intensity of the latter emission decreases by increasing the pH, as the long-lived, deprotonated species dominates the species distribution.

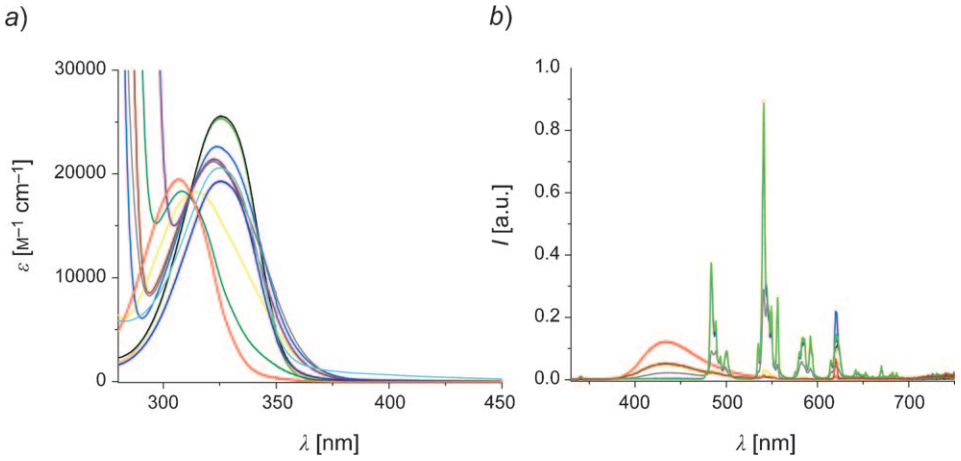

Fig. 4. a) *UV/VIS Absorption spectra of [Tb(***L**^{1}*)] in MeOH as a function of the* pK_a *of the base used.* b) *Luminescence spectra of [Tb(***L**^{1}*)] in MeOH as a function of the* pK_a *of the base used* (λ_{ex} 320 nm) (piperidine (black line), Et_3N (red line), morpholine (geen line), *sym*-collidine (blue line), 2-methyl-1*H*-imidazol (cyan line), $N(CH_2CH(Me)OH)_3$ (royal blue line), 1*H*-benzimidazol (clear blue line), pyridine (dark blue line), pyridin-3-ol (violet line), AcOH (yellow line), $ClCH_2COOH$ (green line), CF_3COOH (orange line)).

Measurements in deuterated solvent enable calculation of '*q*' the number of inner-sphere-bound solvent molecules [30]. These experiments were performed in the presence of piperidine, Et_3N, pyridine, and pyridin-3-ol as buffer bases in CD_3OD and showed a monoexponential decay with identical luminescence lifetimes at high pH (piperidine and Et_3N) and at lower pH (pyridine and pyridin-3-ol). Application of *Beeby*'s equation [31] to MeOH gave 0.0 and 0.3 inner-sphere H_2O molecules (the latter value reflects the protonation of a nearby atom in the complexing ligand when decreasing the pH). This result establishes that there is no MeOH molecule in the inner sphere of the Tb^{III} complexes.

Since **L**^{1} and its complexes are chiral, CD absorption spectra were measured. As shown in *Fig. 6,a*, different spectra were obtained, depending on the pH. In basic medium, the CD spectra reveal two CD exciton bands located at 310 and 335 nm, with positive and negative values, respectively. At neutral pH, the CD spectra only show one main CD exciton band at 335 nm with a positive value. It is interesting to note that, in the case of AcOH or CF_3COOH, a different pattern can be seen with a residual 'complex' absorption at 335 nm for AcOH, while with CF_3COOH (pH 0.2), no remaining transition can be observed at this wavelength (*Fig. 6,a*). In addition, the pH dependence of the Δdeg also suggests the presence of two different species (pH *ca.* 7–8; *Fig. 6,b*).

Also, measurements of circularly polarized luminescence (CPL) to study the chiroptical properties of the Tb^{III}-containing compound were performed. Generally speaking, CPL spectroscopy is the emission analog of CD absorption spectroscopy. CD allows one to detect the differential absorption of left and right circularly polarized lights, while CPL measures the difference in the emission intensity of left and right

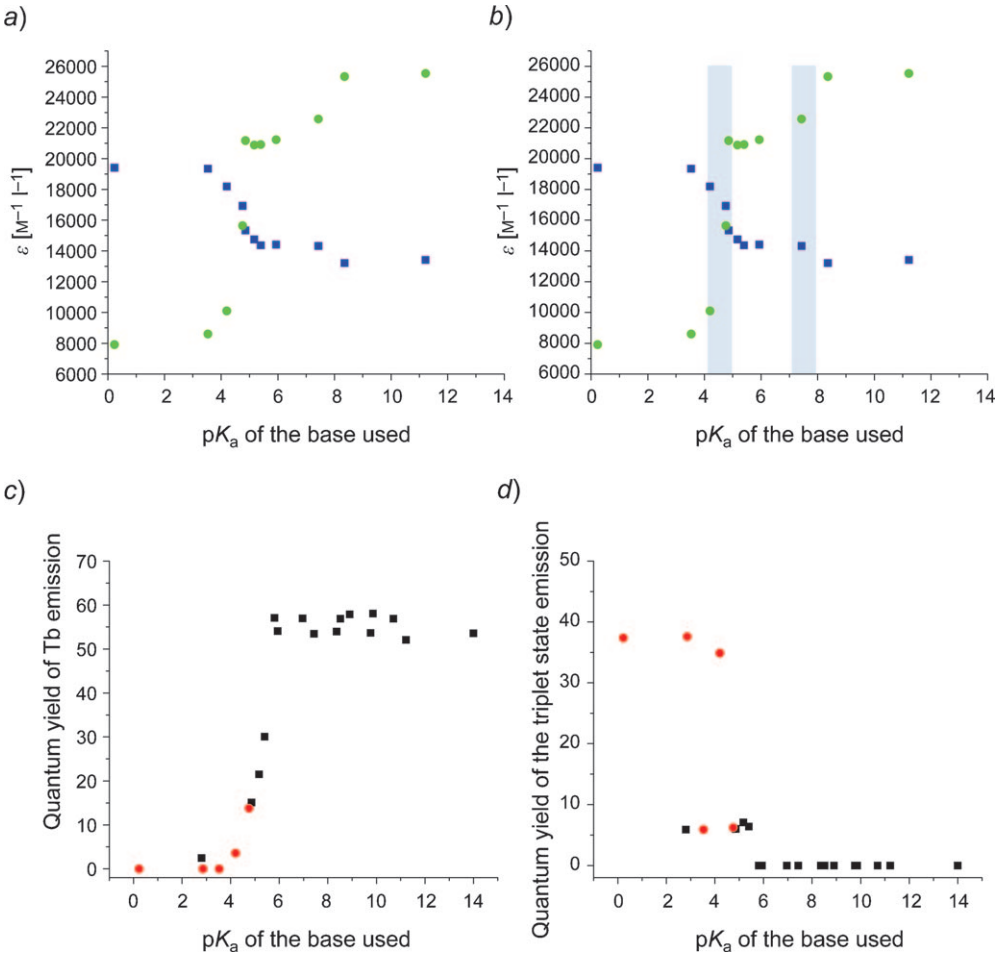

Fig. 5. a) *and* b) *Evolution of the UV/VIS molar absorption coefficient for [Tb(***L**^{1}*)] in MeOH at 306 nm* (■) *and 325 nm* (●) *as a function of the* pK_a *of the base used* (grey bars: changes between species). c) *Evolution of the luminescence quantum yield for [Tb(***L**^{1}*)] as a function of the* pK_a *of the base used* (only based on Tb emission; ■ aprotic 'bases'; ● protic acids). d) *Evolution of the phosphorescence quantum yield for [Tb(***L**^{1}*)] as a function of the* pK_a *of the base used* (only based on residual triplet emission; ■ aprotic; ● protic).

circularly polarized light. With Tb^{III} complexes, the studied transition is the magnetic-dipole-allowed transition $^5D_4 \rightarrow {}^7F_5$ for which one predicts that the CPL would be large [32]. In such measurements, the luminescence dissymmetry ratio, g_{lum}, is defined by *Eqn. 2*, where I_L and I_R refer, respectively, to the intensity of left and right circularly polarized lights.

$$g_{lum} = \frac{\Delta I}{\frac{1}{2}I} = \frac{I_L - I_R}{\frac{1}{2}(I_L + I_R)} \quad (2)$$

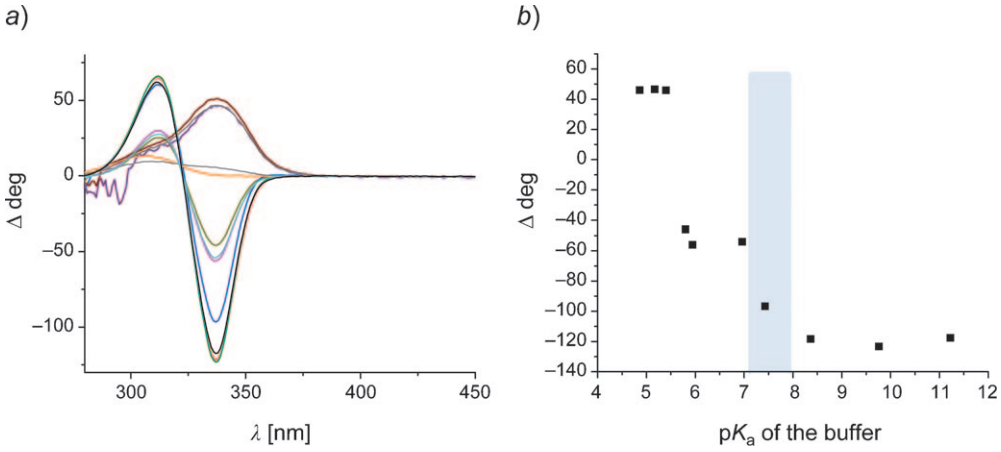

Fig. 6. a) *CD Absorption spectra of [Tb(***L**^{1}**)] in MeOH as a function of the* pK_a *of the base used* (piperidine (black line), Et_3N (red line), morpholine (green line), *sym*-collidine (blue line), 2-methyl-1*H*-imidazol (cyan line), $N(CH_2CH(Me)OH)_3$ (royal blue line), 1*H*-imidazol (brown line), 1*H*-benzimidazol (clear blue line), pyridine (dark blue line), pyridin-3-ol (violet line), AcOH (yellow line), CF_3COOH (orange line)). b) *Evolution of the difference of molar absorption coefficient of [Tb(***L**^{1}**)] in MeOH at 336 nm as a function of the* pK_a *of the base used.*

As can be seen from *Fig. 7*, the CPL spectra of the magnetic-dipole-allowed transition $^5D_4 \rightarrow {}^7F_5$ of [Tb(**L**^{1})] display several peaks corresponding to crystal-field splitting of the electronic level. However, differences in the magnitude, sign, and shape of the CPL signals indicate that the chiral structure of the Tb^{III} complex is dependent on the nature of the base present in solution (*Fig. 7*). It is interesting to note that the CPL activity exhibited by the [Tb(**L**^{1})] complex in the presence of Et_3N (*Fig. 7,a*) is comparable when either a direct excitation of the Tb^{III} ion (λ_{exc} 488 nm) or an indirect excitation through the ligand absorption bands (λ_{exc} 331 nm) is used (*Table 4*). Observation of similar CPL spectra following direct and indirect excitations indicates that the same species in solution is responsible for the CPL activity detected [25]. A useful experiment to determine whether or not the solution contains a mixture of species is to excite directly the Tb^{3+} ion with circularly polarized light. These experiments showed that the g_{lum} values obtained for [Tb(**L**^{1})] in MeOH solution in the presence of Et_3N are independent of the polarization of the excitation beam (*i.e.*, right-, left-, or plane-polarized light). This is consistent with the presence of only one species in solution. If the solution would have contained a mixture of diastereoisomers or enantiomers, the CPL should have been dependent on the excitation polarization [25].

Table 4. *Summary of the CPL Data for [Tb(***L**^{1}**)] in MeOH Solutions*

Complex	Electronic transition	λ [nm]	g_{lum}	Solvent
[Tb(**L**^{1})] (λ_{exc} 331 or 488 nm)	$^5D_4 \rightarrow {}^7F_5$	542.0; 543.0	+0.045; −0.053	1% Et_3N/MeOH
[Tb(**L**^{1})] (λ_{exc} 330 nm)	$^5D_4 \rightarrow {}^7F_5$	542.4; 544.2	+0.043; −0.062	1% pyridine/MeOH
[Tb(**L**^{1})] (λ_{exc} 488 nm)	$^5D_4 \rightarrow {}^7F_5$	543.2; 549.2	+0.051; −0.051	1% pyridine/MeOH

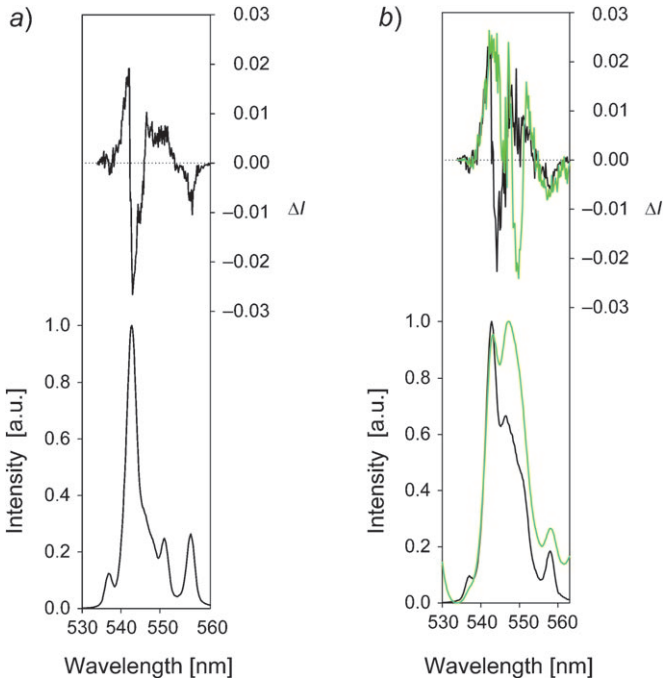

Fig. 7. a) *Circularly polarized luminescence* (upper curve) *and total luminescence* (lower curve) *spectra of the* $^5D_4 \rightarrow {}^7F_5$ *transition of the [Tb(***L**^{1}*)] complex in a* $2.45 \cdot 10^{-5}$ M *MeOH solution* (*O.D.* = 0.6335) *with 1% of* Et_3N *at 295 K, upon excitation at 331 or 488 nm.* b) *Circularly polarized luminescence* (upper curves) *and total luminescence* (lower curves) *spectra of the* $^5D_4 \rightarrow {}^7F_5$ *transition of the [Tb(***L**^{1}*)] complex in a* $2.45 \cdot 10^{-5}$ M *MeOH solution* (*O.D.* = 0.589) *with 1% of pyridine at 295 K, upon excitation at 330* (black) *and 488 nm* (green), *respectively.*

On the other hand, the g_{lum} values obtained for the [Tb(**L**^{1})] complex solution in the presence of pyridine were dependent of the polarization of the excitation beam. In addition, different g_{lum} values were obtained when a direct excitation of the Tb^{III} ion (λ_{exc} 488 nm) and an indirect excitation through the ligand absorption bands (λ_{exc} 330 nm) were used (*Table 4*). These results would suggest that the solution of the [Tb(**L**^{1})] complex contains more than one species responsible for the CPL activity measured when the solution is prepared with pyridine as a base. This is confirmed by the observation of two different CPL spectra when direct and indirect excitations are used (*Fig. 7,b*).

4. *Ytterbium.* Luminescence experiments were also performed with the Yb^{III} ion. Yb is interesting since it is a near-infrared (NIR) emitter which possesses only one excited state ($^2F_{5/2}$). Because of the latter point, the luminescence quantum yield is relatively high for a lanthanide ion emitting in the NIR, thus making the measurement easier than for other NIR emitters. Indeed, the energy gap between the triplet excited state and $^2F_{5/2}$ is large ($\Delta E = 14290\ cm^{-1}$) which makes the energy transfer much less efficient than for the VIS emitters. On the other hand, the absence of excited states between the triplet and $^2F_{5/2}$ avoids any back-transfer-deactivation pathway. The UV/

VIS absorption spectra are identical to the ones of the Tb^{III} and Gd^{III} complexes in the presence of piperidine or pyridin-3-ol.

As can be seen in *Fig. 8,a*, under the most basic conditions (piperidine), the emission spectrum of [Yb(**L**^{1})] is composed of mainly four splittings between 950 and 1150 nm with the most intense at 997 nm. In the presence of a less basic base such as pyridin-3-ol (*Fig. 8,b*), a strikingly different spectrum is obtained with the first splitting as the dominant one (at 975 nm). The spectrum obtained under the latter condition leads to the 'usual' Yb emission as often reported for Yb-based compounds [33–37]. It should be indicated that the profile of the emission spectrum shown in *Fig. 8,a* was already observed for phosphor [38] and also in glass or solid state [33][39]. This

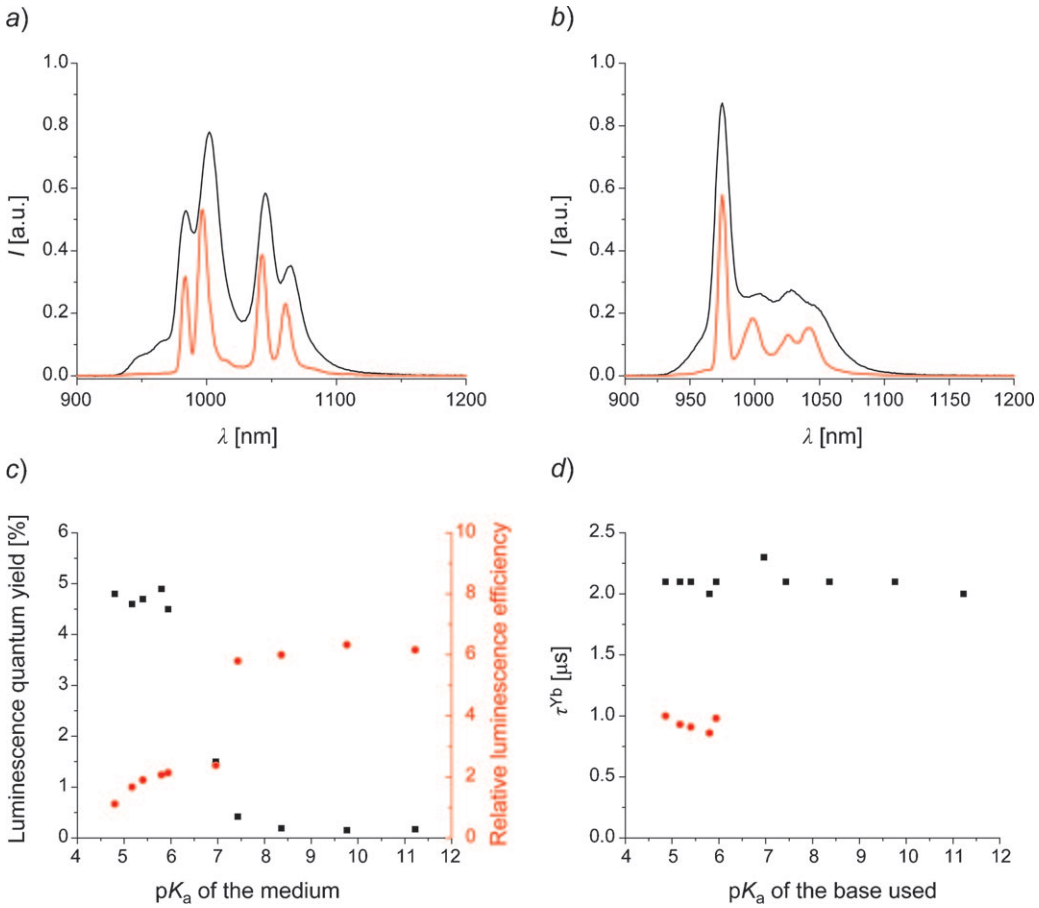

Fig. 8. *Luminescence spectra* a) *of the [Yb(***L**^{1}*)] complex in MeOH in the presence of piperidine in the NIR at room temperature* (black line) *and at 77 K* (red line) *and* b) *of the [Yb(***L**^{1}*)] complex in MeOH in presence of pyridin-3-ol in the NIR at room temperature* (black line) *and at 77 K* (red line) (λ_{ex} 340 nm). c) *Evolution of the luminescence quantum yield in the VIS and of the luminescence relative intensity in the NIR in MeOH as a function of the* pK_a *of the base used for [Yb(***L**^{1}*)].* d) *Evolution of the luminescence excited-state lifetime for [Yb(***L**^{1}*)] as a function of the* pK_a *of the base used.*

suggests an important change of the geometry around the metal as the crystal field changes.

The dependence of the VIS luminescence quantum yield and the Yb emission area as a function of the pH (*Table 5* and *Fig. 8*) were investigated as for the Tb^{III} complex. In the VIS region of the spectrum (*Fig. 8,a*), it can be seen that there is a considerable decrease in luminescence quantum yield at pH > 7.4 (*Fig. 8,c*). Unfortunately, the study of the sensitization process with Yb^{III} is precluded due to the changes observed in the emission profile (emission shifting from the triplet-excited-state to the singlet-excited-state bands). The same phenomenon was observed for the Gd^{III} complex (observation of the emission from the singlet and triplet excited states when basic and acidic conditions were used, see *Table 2*). However, the NIR relative luminescence quantum yield trend (slight increase until 7.4 followed by a considerable jump and then again a slightly increase until reaching a plateau, Fig. S6 of the *S. I.*[2])) clearly supports the presence of two species that certainly possess different geometries around the metal. This hypothesis is also corroborated by the important emission-pattern change observed in the Yb-centered luminescence spectra. It was also confirmed by the pH dependence of the luminescence lifetime of the Yb in the NIR (*Fig. 8,d* and *Table 5*). As for the Tb^{III} complex, a monoexponential decay is observed under basic conditions, whereas two lifetimes can be found when the pH is lower than 7.0. This clearly shows the presence of a second species in solution.

Table 5. *Photophysical Properties of [Yb(***L**^{1}*)] in MeOH with* O.D. *= 0.11*

Buffer	pK_a	$\phi[^3T]$	Efficiency Yb	τ [μs]^{Yb}
Pyridin-3-ol	4.9	0.048	1.0	2.1; 1.0
Pyridine	5.2	0.046	1.5	2.1; 0.93
1*H*-Benzimidazol	5.4	0.047	1.7	2.1; 0.91
1*H*-Imidazol	5.8	0.049	1.85	2.2; 0.86
$N(CH_2CH(Me)OH)_3$	5.9	0.045	1.9	2.1; 0.98
2-Methyl-1*H*-imidazol	7.0	0.015	2.1	2.3
sym-Collidine	7.4	0.0042	5.2	2.1
Morpholine	8.4	0.0019	5.4	2.1
Et_3N	9.8	0.0015	5.7	2.1
Piperidine	11.2	0.0017	5.5	2.3

To understand the striking difference of emission patterns, the Yb^{III} complex of the isophthalamide-based ligand H_2**L**^{2} (*Fig. 1*) was prepared. As can be seen in *Fig. 9*, the emission of $[Yb(\mathbf{L}^{2})_2]^-$ is composed of a main splitting at 977 nm followed by a broad shoulder (much less intense). This emission profile looks like the emission of [Yb(**L**^{1})] in the presence of pyridin-3-ol as a base. This suggests that at low pH, the complex existing in solution is based on the 2-hydroxybenzamide units (no involvement of the cyclen unit) while, at high pH, the different spectrum seems to indicate that not only the 2-hydroxybenzamide moieties but all or part of the cyclen moiety would participate to the complexation.

To ensure that the result is not just coincidential, measurements in methanol (CD_3OD, MeOD, and MeOH) were performed, and all the results are reported in *Table 6*. As already discussed, the decay found for [Yb(**L**^{1})] is biexponential in the

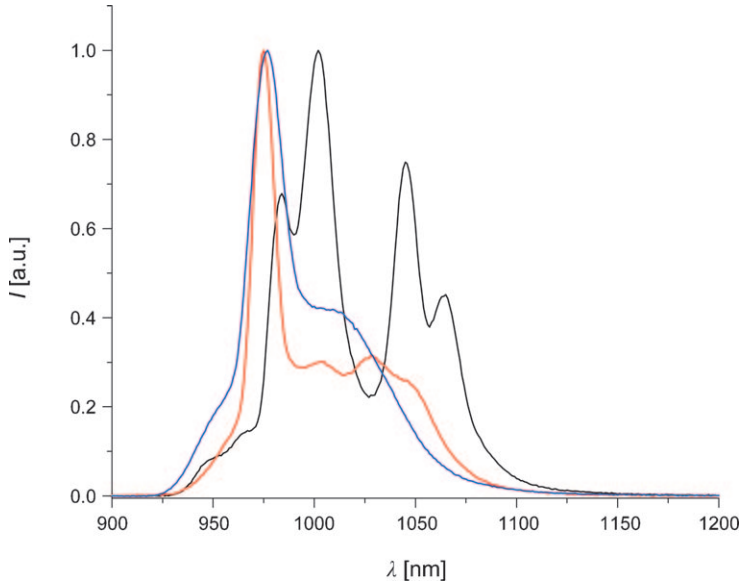

Fig. 9. *Luminescence spectrum of [Yb(**L**^{1})] with piperidine as a base* (black line) *and [Yb(**L**^{1})] with pyridin-3-ol as a base* (red line) *and of [Yb(**L**^{2})$_2$]$^-$ with piperidine or pyridin-3-ol as a base* (blue line) (in MeOH at room temperature, λ_{ex} 320 nm).

presence of pyridin-3-ol as a base with a component at *ca.* 2 μs and another one at *ca.* 1 μs in undeuterated MeOH. The longer luminescence lifetime possesses a small weight as compared to the other one. It can also be found that the value of the relative luminescence quantum yield is identical (within the experimental error) to the one of [Yb(**L**^{1})] in the presence of piperidine as a base. Interestingly, the shorter luminescence lifetime (1 μs) is close to that of [Yb(**L**^{2})$_2$]$^-$ (*Table 6*). In MeOD and CD_3OD, the same kind of trend can be found. These results seem to confirm the fact that the complex formed mainly involves the 2-hydroxybenzamide chromophores at low pH, whereas stronger bases certainly allow involvement of the cyclen moiety in lanthanide coordination. Thus, this yields different properties than for the 'pure' isophthalamide-based complexes.

Table 6. *Luminescence Lifetime of [Yb(**L**^{1})] and [Yb(**L**^{2})$_2$]$^-$ Emission in MeOH, MeOD, and CD_3OD*

	MeOH	MeOD	CD_3OD
	τ [μs]	τ [μs]	τ [μs]
[Yb(**L**^{1})] (piperidine)	2.15	5.90	6.65
[Yb(**L**^{1})] (pyridin-3-ol)	2.30; 1.05	5.80; 13.90	6.60; 17.10
[Yb(**L**^{2})$_2$]$^-$	1.00	12.90	21.40

The number of MeOH molecules in the inner sphere (n) can be calculated with the formula developed for Yb^{III} by *Beeby et al.* [40] adapted to MeOH. This formula was defined in H_2O with different kinds of ligand. Since the measurements were made in

H_2O, no C–H vibrations are brought by the solvent and, in consequence, this kind of vibration has not been taken into account. For [Yb($\mathbf{L^1}$)], it can be found that, in piperidine, the complex does not have any solvent molecules in the inner sphere, while, at lower pH, the calculation suggests that there would be one molecule of solvent bound to the metal ($n = 0.8$) which is in contradiction with the data obtained for [Tb($\mathbf{L^1}$)]. This result certainly reflects the larger influence of the medium (OH, NH, and CH vibrations) on the luminescence properties for Yb-based emission *vs.* Tb-based emission (VIS emitter).

5. *Europium.* A reasonable level of sensitization was expected with Eu^{III} because the triplet excited state is higher than the $^5D_2$ state (too high to be optimum) [41][42]. Instead, as illustrated in *Fig. 10,a*, only the triplet-excited-state emission could be recorded. Therefore, at 77 K, the 'typical' and characteristically split spectrum of Eu was observed (*Fig. 10*).

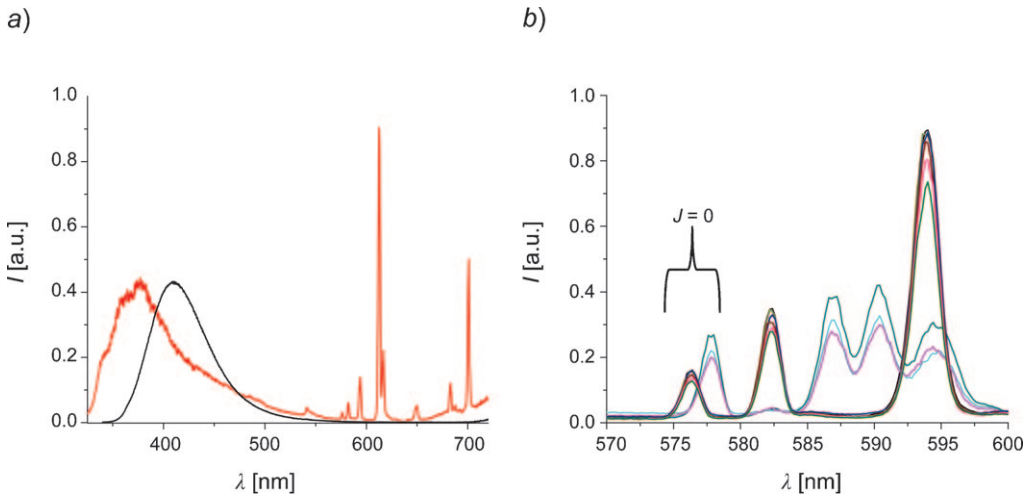

Fig. 10. a) *Luminescence spectrum of [Eu($\mathbf{L^1}$)] in the VIS in MeOH containing 1% of piperidine at room temperature* (λ_{ex} 340 nm; black line) *and at 77 K* (λ_{ex} 320 nm; red line). b) *Focus on the* J = *0 and* J = *1 of the luminescence spectrum of [Eu($\mathbf{L^1}$)] in the VIS in MeOH/EtOH 1:4 at 77 K containing 1% of piperidine* (black line), *of Et$_3$N* (red line), *of morpholine* (blue line), *of* sym-*collidine* (green line), *of 1*H-*imidazol* (dark green line), *of pyridine* (cyan line), *and of pyridin-3-ol* (violet line) (λ_{ex} 320 nm).

The recovery of the sensitization occurring at 77 K strongly suggests that there is a transfer–back-transfer interaction between the triplet excited state of the ligand and the $^5D_2$ of the Eu^{3+} ion with a much faster triplet-excited-state relaxation (radiative and nonradiative) than the $^5D_2 \rightarrow {}^5D_0$ relaxation.

At 77 K in solid matrix, a thorough study of the basicity dependence reveals two different patterns if one examines the $J = 0$ and $J = 1$ transitions (*Fig. 10,b*). Interestingly, only one $J = 0$ transition can be seen under all conditions, suggesting the presence of only one species. Also, no spectral differences are observed at pH higher or lower than 5.8, again suggesting the presence of only one species. Noticeably, a luminescence-lifetime experiment at 77 K confirmed the presence of only one species

in every case: at high pH, a luminescence lifetime of 720 μs can be observed, while under mildly basic conditions, a luminescence lifetime of 650 μs is measured.

These experiments on [Eu(**L**^{1})] also establish the presence of two emissive species: one existing at high pH, the other one present at pH lower than 7. In the following part, the best conditions of sensitization were used to sensitize other lanthanide ions.

6. *Pr, Nd, Sm, Dy, and Tm.* Because the ligand triplet-excited-state energy seems well suited to populate most of the Ln^{III} cations, all the lanthanide complexes of **L**^{1} emitting from the f–f orbitals were prepared, yielding sensitization of Pr, Nd, Sm, Dy, and Tm. With the exception of Nd, which only possesses transitions in the NIR region, all these lanthanide ions emit in both the NIR and VIS regions. All the relevant luminescence spectra of the complexes in the VIS and in the NIR regions are presented in *Fig. 11*, and a brief description of these luminescence spectra is provided below.

For Pr^{III}, the $^3P_0$ (21750 cm^{-1}) is populated yielding transitions attributed to the $^1D_2 \rightarrow {}^3H_4$ (*Fig. 11,a*), $^1D_2 \rightarrow {}^3F_3$, and $^1D_2 \rightarrow {}^3F_4$ transitions (*Fig. 11,b*).

Nd^{III} is also sensitized by ligand **L**^{1} resulting in the typical emission feature of this ion (Fig. S7 of the *S. I.*[2])) with the $^4F_{3/2} \rightarrow {}^4I_{11/2}$ and $^4F_{3/2} \rightarrow {}^4I_{13/2}$ transitions in the NIR.

For Sm^{III}, the $^4G_{5/2}$ excited state emits in the VIS (*Fig. 11,c*) and in the NIR region where three transitions can be observed (*Fig. 11,d*), and arising from the $^4G_{5/2}$ level to the $^6F_{5/2}$, $^6F_{7/2}$, and $^6F_{9/2}$, respectively.

Dy^{III} emits from the $^4F_{9/2}$ excited state giving rise to four transitions to the $^6H_{15/2}$, $^6H_{13/2}$, $^6H_{11/2}$, and $^6H_{9/2}/{}^6F_{11/2}$ in the VIS (*Fig. 11,e*) and three transitions in the NIR (*Fig. 11,f*) attributed to the $^4F_{9/2} \rightarrow {}^7F_{7/2}$, $^4F_{9/2} \rightarrow {}^7F_{5/2}$, and $^4F_{9/2} \rightarrow {}^7F_{3/2}$.

Tm^{III} emission from the $^1G_4$ level is observed with the $^1G_4 \rightarrow {}^3H_6$ and the $^1G_4 \rightarrow {}^3H_4$ transitions in the VIS (*Fig. 11,g*) and the $^1G_4 \rightarrow {}^3F_4$ in the NIR (*Fig. 11,h*).

Conclusions. – In conclusion, the synthesis of a cyclen derivative containing four 2-hydroxybenzamide groups, H_4**L**$^1 \cdot 2$ HBr, is described. The spectroscopic properties of the Ln^{III} complexes of **L**^{1} (Ln = Gd, Tb, Yb, and Eu) were studied and reveal that at least two species are present in solution whose relative populations are dependent on the pH. In basic medium, an intense long-lived emission is observed (for [Tb(**L**^{1})] and [Yb(**L**^{1})]), while in mildly basic medium, a weaker emission of a shorter-lived species is present. A study of the $J = 0$ and $J = 1$ transition patterns of the [Eu(**L**^{1})] emission also supports the change in species upon protonation of the complexing ligand. These two different complexes change their coordination geometry upon protonation/deprotonation of one of the twelve coordinating atoms (eight O-atoms and four N-atoms), but in both cases still exclude solvent molecules from the inner coordination sphere. This was also supported by the lifetime and CPL measurements with some of the Ln^{III} complexes of interest.

In addition, under the more basic conditions (the most efficient conditions for sensitization of Tb^{III} and Yb^{III}), other lanthanides(III) (Pr^{III}, Nd^{III}, Sm^{III}, Dy^{III}, and Tm^{III}) were sensitized showing emission in the NIR region (and in the VIS in some cases). All emissive transitions on the spectra were attributed.

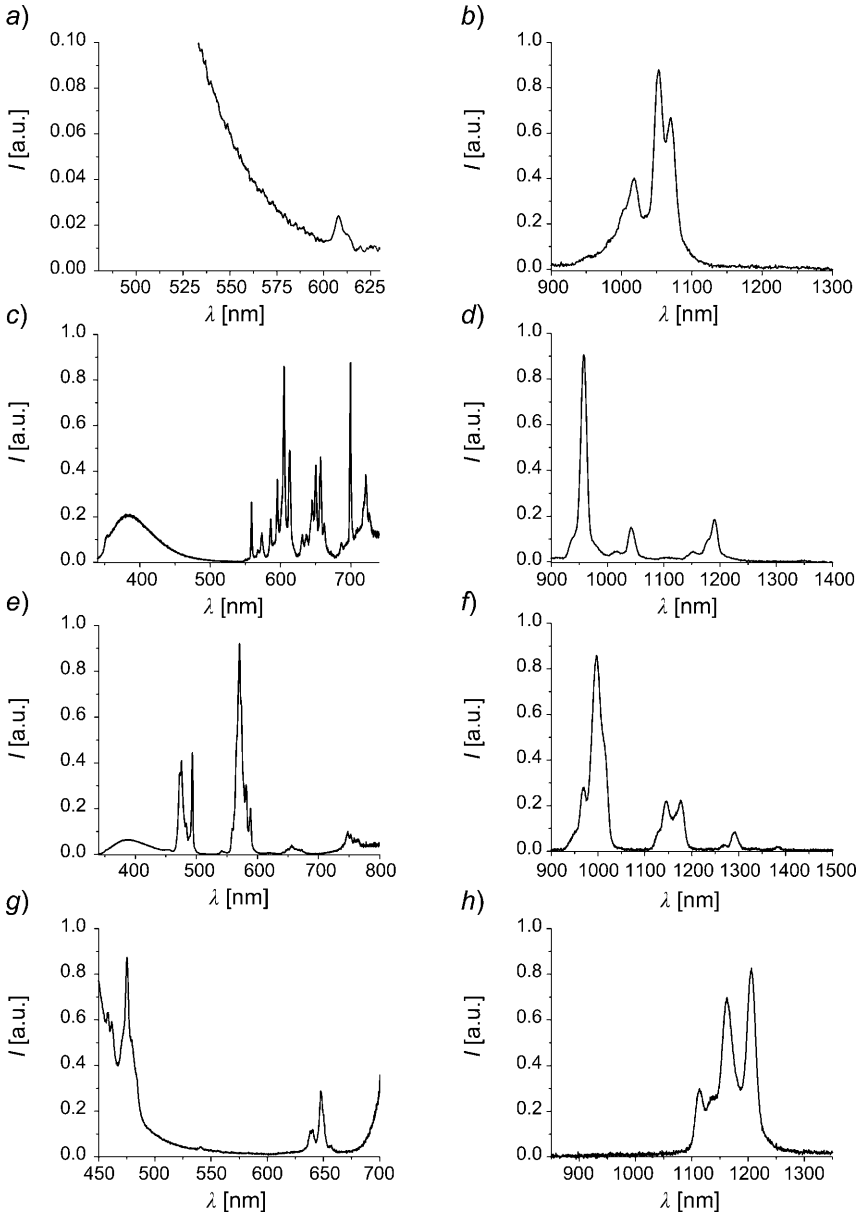

Fig. 11. *Luminescence spectrum in MeOH containing 1% of piperidine of* a*) [Pr(***L**^{1}*)] in the VIS,* b*) [Pr(***L**^{1}*)] in the NIR,* c*) [Sm(***L**^{1}*)] in the VIS,* d*) [Sm(***L**^{1}*)] in the NIR,* e*) [Dy(***L**^{1}*)] in the VIS,* f*) [Dy(***L**^{1}*)] in the NIR,* g*) [Tm(***L**^{1}*)] in the VIS, and* h*) [Tm(***L**^{1}*)] in the NIR* (λ_{ex} 340 nm).

This work was partially supported by the *NIH* (Grant HL69832) and supported by the Director, *Office of Science*, *Office of Basic Energy Sciences*, and the *Division of Chemical Sciences, Geosciences, and Biosciences* of the *U.S. Department of Energy* at the *Lawrence Berkeley National Laboratory*

(*LBNL*) under Contract No. DE-AC02-05CH11231. This technology is licensed to *Lumiphore, Inc.* in which some of the authors have a financial interest. *G. M.* thanks the *National Institute of Health, Minority Biomedical Research Support* (2 S06 GM008192-27) and the *Henry Dreyfus Teacher Scholar Award* for financial support.

REFERENCES

[1] H. L. Handl, R. J. Gillies, *Life Sci.* **2005**, *77*, 361.
[2] S. Petoud, S. M. Cohen, J.-C. G. Bünzli, K. N. Raymond, *J. Am. Chem. Soc.* **2003**, *125*, 13324.
[3] B. Song, G. Wang, M. Tan, J. Yuan, *J. Am. Chem. Soc.* **2006**, *128*, 13442.
[4] S. M. Borisov, O. S. Wolbeis, *Anal. Chem.* **2006**, *78*, 5094.
[5] M. I. Stich, S. Nagl, O. S. Wolbeis, U. Henne, M. Schaeferling, *Adv. Funct. Mater.* **2008**, *18*, 1399.
[6] D. Parker, *Coord. Chem. Rev.* **2000**, *205*, 109.
[7] M. S. Tremblay, M. Halim, D. Sames, *J. Am. Chem. Soc.* **2007**, *129*, 7570.
[8] J. Kido, Y. Okamoto, *Chem. Rev.* **2002**, *102*, 2357.
[9] T.-S. Kang, B. S. Harrison, T. J. Foley, A. S. Knefely, J. M. Boncella, J. R. Reynolds, K. S. Schanze, *Adv. Mater.* **2003**, *15*, 1093.
[10] A. de Bettencourt-Dias, *Dalton Trans.* **2007**, 2229.
[11] K. Kuriki, Y. Koike, Y. Okamoto, *Chem. Rev.* **2002**, *102*, 2347.
[12] H. K. Kim, S. G. Roh, K.-S. Hong, J.-W. Ka, N. S. Baek, J. B. Oh, M. K. Nah, Y. H. Cha, J. Ko, *Macromol. Res.* **2003**, *11*, 133.
[13] P. Escribano, B. Julián-López, J. Planelles-Aragó, E. Cordoncillo, B. Viana, C. Sanchez, *J. Mater. Chem.* **2008**, *18*, 23.
[14] J. K. R. Weber, J. J. Felten, B. Cho, P. C. Nordine, *Nature (London)* **1998**, *393*, 769.
[15] L. H. Slooff, A. Polman, S. I. Klink, G. A. Hebbink, L. Grave, F. C. J. M. van Veggel, D. N. Reinhoudt, J. W. Hofstraat, *Opt. Mater.* **2000**, *14*, 101.
[16] L. H. Slooff, A. van. Blaaderen, A. Polman, G. A. Hebbink, S. I. Klink, F. C. J. M. van Veggel, D. N. Reinhoudt, J. W. Hofstraat, *J. Appl. Phys.* **2002**, *91*, 3955.
[17] S. Moynihan, R. Van Deun, K. Binnemans, J. Krueger, G. von Papen, A. Kewell, G. Crean, G. Redmond, *Opt. Mater.* **2007**, *29*, 1798.
[18] G. Pintacuda, M. John, X.-C. Su, G. Otting, *Acc. Chem. Res.* **2007**, *40*, 206.
[19] W. G. Perkins, G. A. Crosby, *J. Chem. Phys.* **1965**, *42*, 407.
[20] W. G. Perkins, G. A. Crosby, *J. Chem. Phys.* **1965**, *42*, 2621.
[21] A. P. S. Samuel, J. Xu, K. N. Raymond, *Inorg. Chem.* **2009**, *48*, 687.
[22] A. Beeby, L. M. Bushby, D. Maffeo, J. A. G. Williams, *J. Chem. Soc., Dalton Trans.* **2002**, 48.
[23] M. H. V. Werts, R. T. F. Jukes, J. W. Verhoeven, *Phys. Chem. Chem. Phys.* **2002**, *4*, 1542.
[24] S. D. Bonsall, M. Houcheime, D. A. Straus, G. Muller, *Chem. Commun.* **2007**, 3676.
[25] K. Do, F. C. Muller, G. Muller, *J. Phys. Chem. A* **2008**, *112*, 6789.
[26] G. A. Crosby, J. N. Demas, *J. Phys. Chem.* **1971**, *75*, 991.
[27] E. G. Moore, J. Xu, C. J. Jocher, E. J. Werner, K. N. Raymond, *J. Am. Chem. Soc.* **2006**, *128*, 10648.
[28] E. G. Moore, J. Xu, C. J. Jocher, I. Castro-Rodriguez, K. N. Raymond, *Inorg. Chem.* **2008**, *47*, 3105.
[29] A. D'Aléo, J. Xu, E. G. Moore, C. J. Jocher, K. N. Raymond, *Inorg. Chem.* **2008**, *47*, 6109.
[30] R. C. Holz, C. A. Chang, W. D. Horrocks, *Inorg. Chem.* **1991**, *30*, 3270.
[31] A. Beeby, I. M. Clarkson, R. S. Dickins, S. Faulkner, D. Parker, L. Royle, A. S. de Sousa, J. A. G. Williams, M. Woods, *J. Chem. Soc., Perkin Trans. 2* **1999**, 493.
[32] J. P. Riehl, G. Muller, 'Handbook on the Physics and Chemistry of Rare Earths', Eds. K. A. Gschneidner, J.-C. G. Bünzli, and V. K. Pecharsky, North-Holland Publishing, Amsterdam, 2005.
[33] J. X. Meng, K. F. Li, J. Yuan, L. L. Zhang, W. K. Wong, K. W. Cheah, *Chem. Phys. Lett.* **2000**, *332*, 313.
[34] S. Faulkner, A. Beeby, M.-C. Carrié, A. Dadabhoy, A. M. Kenwright, P. G. Sammes, *Inorg. Chem. Commun.* **2001**, *4*, 187.
[35] A. Beeby, R. S. Dickins, S. Faulkner, D. Parker, J. A. G. Williams, *Chem. Commun.* **1997**, 1401.

[36] N. M. Shavaleev, L. P. Moorcraft, S. J. A. Pope, Z. R. Bell, S. Faulkner, M. D. Ward, *Chem. – Eur. J.* **2003**, *9*, 5283.
[37] G. S. Kottas, M. Mehlstäubl, R. Fröhlich, L. De Cola, *Eur. J. Inorg. Chem.* **2007**, 3465.
[38] W. Ryba-Romanowski, S. Golb, *J. Mol. Struct.* **1998**, *450*, 223.
[39] J. Le Person, V. Nazabal, R. Balda, J.-L. Adam, J. Fernández, *Opt. Mater.* **2005**, *27*, 1748.
[40] S. Faulkner, A. Beeby, R. S. Dickins, D. Parker, J. A. G. Williams, *J. Fluorescence* **1999**, *9*, 1095.
[41] M. Latva, H. Takalo, V.-M. Mukkala, C. Matachescu, J. C. Rodriguez-Ubis, J. Kankare, *J. Lumin.* **1997**, *75*, 149.
[42] A. D'Aléo, A. Picot, A. Beeby, J. A. G. Williams, B. Le Guennic, C. Andraud, O. Maury, *Inorg. Chem.* **2008**, *47*, 10258.

Received May 4, 2009